PROCEEDINGS OF SCIENCE

Compton Scattering from ^{3}He using an Active Target

John R.M. Annand*, **Bruno Strandberg**
University of Glasgow, Scotland UK
E-mail: john.annand@glasgow.ac.uk

Hans-Juergen Arends, Andreas Thomas

University of Mainz, Germany

Evie Downie

The George Washinton University, USA

David Hornidge, Meg Morris

Mount Allison University, Canada

Vahe Sokoyan

University of Mainz, Germany and The George Washington University, USA

An new technique to measure Compton scattering on ^{3}He is described. It will use the tagged photon beam at the MAMI facility in Mainz. Scattered photons will be detected in the CB/TAPS electromagnetic calorimeter, in coincidence with the recoiling ^{3}He detected in the active target, which is a high pressure He gas scintillator. The method to separate the weak Compton signal from background is presented, along with an estimate of the obtainable experimental uncertainty.

The 8th International Workshop on Chiral Dynamics
29 June 2015 - 03 July 2015
Pisa, Italy

*Speaker.

PoS(CD15)092

1. Introduction

The determination of the nucleon polarisabilities is a major component of the physics program at the tagged-photon hall of the MAMI accelerator in Mainz. Recently there have been major advances at Mainz in obtaining both the scalar and spin polarisabilities of the proton, with the first double polarised measurement of Σ_{2x} yielding the first direct means to access γ_{E1E1}. However information on neutron polarisabilities remains extremely fragmentary. The scalar polarisabilities are poorly known compared to the proton and the spin polarisabilities are almost entirely unknown. Recently the $\gamma+^2H \rightarrow \gamma+^2H$ reaction has been measured at MAX-lab and a Chiral Effective Field Theory (χEFT) analysis of the new, extended world data set has reduced the uncertainties in α^n_{M1} and β^n_{M1} significantly. However it will be important to extend these results using an alternative experimental technique. We have developed a He gas scintillator active target for photo-reaction measurements at MAX-lab and, based on this experience, a new target is being built for the tagged photon facility at Mainz. There it will measure $\gamma+^3He \rightarrow \gamma+^3He$ and $\gamma+^4He \rightarrow \gamma+^4He$, in conjunction with the Crystal Ball and TAPS detectors.

1.1 Motivation

Compton scattering $\gamma N \rightarrow \gamma N$, [1,2] is an extremely "clean" probe of the response of low-energy nucleon degrees-of-freedom, since both initial- and final-state interactions are electromagnetic and can be calculated perturbatively. Its importance is recognised in the 2007 NSAC/DOE and 2010 NuPECC Long-Range Plans [3,4] which emphasise the need to improve the proton, deuteron and ^{3}He database. At Mainz there is already a highly successful programme of Compton scattering experiments on the proton [5,6,7] with both polarised and unpolarised beams and targets.

Polarisabilities arise because the electric and magnetic fields of the photon displace the charged constituents of a hadron and thus induce many charge and current multipoles, which radiate with characteristic angular distributions. The polarisabilities are the energy-dependent factors between each photon field and the corresponding induced radiation multipole moment. Each parametrises the response of the internal degrees-of-freedom (with particular quantum numbers) with respect to deformations of a given electric or magnetic multipolarity at energy ω. Each interaction of the hadronic constituents is characterised by a specific energy- and angle-dependence of the emitted radiation, which can be disentangled in the differential Compton scattering cross section $\sigma(\omega,\theta)$.

A multipole analysis produces coefficients which are the energy-dependent nucleon polarisabilities. They measure the stiffness of the low-energy degrees of freedom of a nucleon (spin $\frac{\vec{\sigma}}{2}$) against transitions $X_l \rightarrow Y_{l'}$ ($l' = l \pm \{0;1\}$; $X,Y = E,M$) of definite multipolarity, in the electromagnetic field of a real photon of frequency ω. The effective interaction Hamiltonian up to third order may be written as:

$$H_{eff} = 2\pi\{\alpha_{E1}(\omega)\vec{E}^2 + \beta_{M1}(\omega)\vec{B}^2 + \gamma_{E1E1}(\omega)\vec{\sigma}\cdot(\vec{E}\times\dot{\vec{E}}) \qquad (1.1)$$
$$+\gamma_{M1M1}(\omega)\vec{\sigma}\cdot(\vec{B}\times\dot{\vec{B}}) - 2\gamma_{M1E2}(\omega)\sigma^i B^j E_{ij} + 2\gamma_{E1M2}(\omega)\sigma^i E^j B_{ij}\}.$$

This dipole approximation of the response of the nucleon, valid for $\omega \lesssim 300$ MeV, is characterised by six linearly independent polarisabilities. Two spin-independent (scalar) polarisabilities, $\alpha_{E1}(\omega)$ and $\beta_{M1}(\omega)$, parametrise electric and magnetic dipole transitions and for the proton they

are relatively well determined. A recent χEFT analysis [8] has produced the values $\alpha^p_{E1}(0) \approx 10.65 \pm 0.35(\text{stat}) \pm 0.2(\text{BSR}) \pm 0.3(\text{Th})$, $\beta^p_{M1}(0) \approx 3.15 \pm 0.35(\text{stat}) \pm 0.2(\text{BSR}) \pm 0.3(\text{Th})$, in units of 10^{-4} fm^3, where (stat) refers to the uncertainty in the fitting procedure, (BSR) the incertainty resulting from a Baldin-Sum-Rule constraint on the fit and (Th) the uncertainty in the theoretical interpretation. For the neutron, α^n_{E1} and β^n_{M1} are known much less precisely.

The relatively unknown spin polarisabilities parametrise the response of the nucleon spin. $\gamma_{E1E1}(\omega)$ and $\gamma_{M1M1}(\omega)$ describe how the electromagnetic field associated with the spin degrees-of-freedom produces a birefringence effect in the nucleon. An incoming photon causes a dipole deformation in the nucleon spin, which in turn leads to dipole radiation, related to its axis. The two mixed spin polarisabilities, $\gamma_{E1M2}(\omega)$ and $\gamma_{M1E2}(\omega)$, relate to scattering where the angular momenta of the incident and outgoing photons differ by one unit.

χEFT predicts that small proton–neutron differences stem from chiral-symmetry breaking interactions of the pion cloud around the nucleon and therefore probe the symmetries of QCD directly. However neutron information to date is fragmentary. Experimentally the target neutron must be bound in a light nucleus, which complicates the polarisability analysis. On the other hand, this provides the opportunity to couple to the charged meson-exchange currents which bind the nucleus together. Around pion-production threshold one can also study the transition to a dynamical Δ, to understand better its role not only for nucleons, but also for few-body nuclei.

1.1.1 Neutron Compton Scattering

For the proton, the electric and magnetic polarisabilities have a relatively pronounced effect on the cross section, due to interference with the Thomson amplitude. For a free neutron, there is no Thomson term, so the effect of the polarisabilities on the cross section is smaller, and consequently (quasi-free) neutron Compton scattering was for many years not considered to be feasible experimentally. An alternative technique to extract polarisabilities from electromagnetic scattering of ~ 600 keV neutrons in the Coulomb field of enriched ^{208}Pb [9] has been used. However there are sizeable systematic uncertainties in this procedure and the actual size of the uncertainties is disputed.

Lacking a free neutron target, almost all of the information on the neutron polarisabilities, α^n_{E1} and β^n_{M1}, comes from Compton scattering on the deuteron. Quasi free $\gamma + ^2H \rightarrow \gamma + n + p$, where the proton is a spectator, has been used to approximate free scattering and pioneering work [10] was performed at Mainz. However there was considerable model dependence in the extraction of $\alpha^n_{E1}, \beta^n_{M1}$ from sub-pion-threshold data and further experiments were performed at somewhat higher energies at SAL [11] and Mainz [12]. The Mainz experiment covered the incident energy range $\omega = 200 - 400$ MeV and measured $\gamma' - n$ coincidences using the CATS NaI gamma spectrometer and a neutron time-of-flight array.

Given knowledge of the proton polarisabilites, the neutron polarisabilities can be extracted from the isospin-averaged nucleon polarisabilities obtained from elastic Compton scattering on the deuteron. The dependence of the cross section on isospin-averaged polarizabilities is enhanced strongly, compared with Compton scattering by free neutrons, due to interference with the Thomson amplitude. On the other hand, bound nucleons require consideration of coupling to meson exchange currents and the $n - p$ interaction in the intermediate state. Experimentally the technique

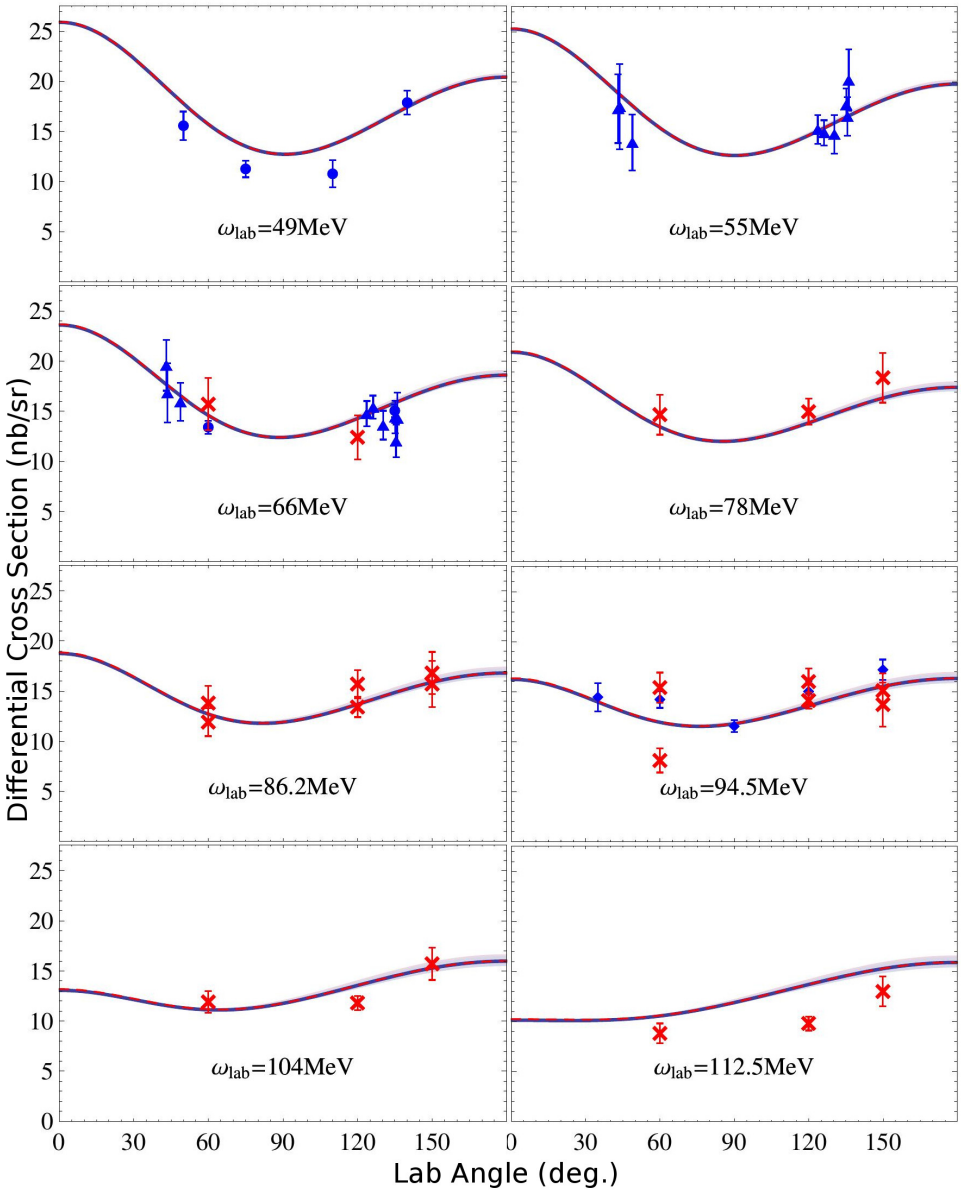

Figure 1: The differential cross section for Compton scattering on the deuteron.

requires very good γ' energy resolution to separate elastic scattering from the breakup channel (2.2 MeV separation).

The world $\gamma+^2H \rightarrow \gamma+^2H$ data set is shown in Fig.1. Following a pioneering Illinois experiment [13] (blue circle), differential cross sections for Compton scattering from the deuteron were measured at MAX-Lab [14] (blue triangle) and SAL [15] (blue diamond at $\omega_{lab} = 94.5$ MeV). Most recently, a new MAX-lab experiment [16] (red cross) has been performed at incident energies $\omega = 67 - 116$ MeV and scattering angles $\theta_\gamma = 60, 90, 120, 150^\circ$, using three very large

NaI spectrometers. A χEFT analysis of the world data set [16] (curves Fig. 1) has produced $\alpha^n_{E1} = 11.55 \pm 1.25(stat) \pm 0.2(BSR) \pm 0.8(Th)$, $\beta^n_{M1} = 3.65 \pm 1.25(stat) \pm 0.2(BSR) \pm 0.8(Th)$.

No Compton scattering data exists for the He isotopes, but there have been a measurements on ^6Li at the HIγS facility [17] and MAX-lab [18]. Extension of a theoretical framework [19] to interpret Compton scattering on light nuclei is under investigation

He isotopes (Z=2) have a significantly larger Compton scattering cross section than the deuteron (Z=1) and at 120 MeV the cross section scales as $\sim Z$. In He, interference of the proton Thomson terms with the neutron polarisability amplitudes produces a greater sensitivity of the differential cross section to the polarisabilities. Experiments at lower energies are easier to interpret theoretically although the sensitivity to the polarisabilities increases with energy. However, before this stage is reached, it is important to test χEFT predictions of the ^{3}He differential cross section which are relatively undeveloped due to a complete lack of data.

Fig.2 (top) displays the calculation made by Shukla *et al.* [20] for $\gamma + {}^3He \rightarrow \gamma + {}^3He$, using Heavy-Baryon χPT ($HB\chi PT$) to order $\mathcal{O}(e^2Q)$. These calculations represent a first step and extension to $\mathcal{O}(e^3Q^2)$, with explicit inclusion of the Δ would be highly desirable. New calculations for ^{3}He, which include dynamical Δ contributions, have been made recently [21]. Although small at 60 MeV, the effect of this extension is sizeable by 120 MeV (Fig. 2).

2. Experimental Method

We plan to measure the double differential cross section $\sigma(\omega, \theta_\gamma)$ for Compton scattering on ^{3}He (and ^{4}He), in the energy range $\omega = 80 - 200$ MeV, with sufficient precision to extract values of the isospin averaged polarisabilities $\alpha^s_{E1}, \beta^s_{M1}$. Extraction will be preformed using a χEFT fit to the angular distributions, which will be binned in 10 MeV intervals of ω and in 0.2 intervals of $\cos\theta_\gamma$. With 110 data points, the energy and angular definition of the present experiment will be superior to previous experiments on the deuteron (Fig. 1), placing tighter constraints on fitting procedures. The experiment will take place at the Mainz tagged-photon facility using the Glasgow-Mainz photon tagger, the $\sim 4\pi$ Crystal-Ball (CB) and TAPS electromagnetic calorimeters to detect the γ' and a high-pressure He gas-scintillator Active Target (AT) to detect the recoiling He nucleus.

The experiment will employ an unpolarised photon beam produced by bremsstrahlung on a $10\,\mu m$ Cu radiator. The bremsstrahlung is momentum tagged in the tagged-photon spectrometer [22], which is a broad-band dipole covering $\sim 5 - 95\%$ of E_0, the energy of the primary electron beam. At $E_0 = 855$ MeV, the minimum tagged-photon energy is $\lesssim 50$ MeV, extending up to$\sim$ 795 MeV and the average energy width per channel of the focal-plane detector is ~ 2 MeV. An upgrade to the spectrometer's focal plane detector is planned, which will produce a factor ~ 4 increase in tagged-photon intensity.

This experiment will use a new version of the high-pressure gas-scintillator AT (Fig.3), developed originally for photonuclear experiments at MAX-lab [23]. The target operates at a pressure of 2 MPa and an active length of 400 mm produces an overall thickness of $0.15\,g.cm^{-2}$ for ^{4}He. It consists of a cylindrical active region read out by up to 128 Si photomultipliers (SiPMT).

Scintillations in pure He fall mainly in the vacuum UV region, which is difficult to detect efficiently, so that they are shifted to ~ 420 nm by addition of ~ 500 ppm N_2. This addition also produces a sharp signal which is beneficial in terms of timing precision and freedom from pile

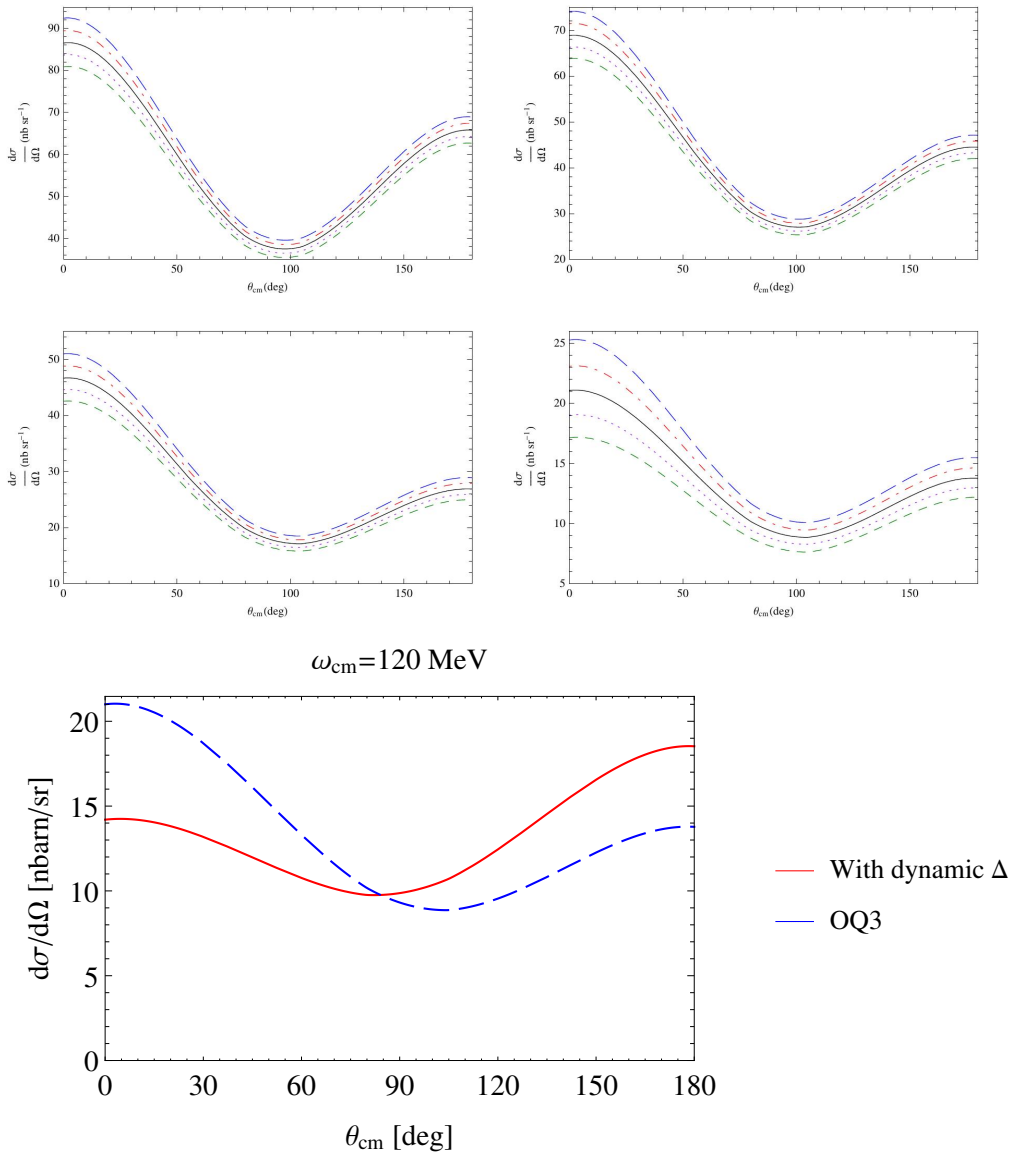

Figure 2: Calculation of the $\gamma + ^3He \rightarrow \gamma + ^3He$ differential cross section showing the dependence on α^n_{E1} (top 4 plots). upper-left 60 MeV, upper-right: 80 MeV, lower-left: 100 MeV, lower-right: 120 MeV. Curves top: full $\Delta\alpha^n_{E1}$ =0, long-dash =-4; dot-dash =-2; dot =+2; dash =+4. Bottom plot: comparison of the differential cross section at 120 MeV with (full red line) and without (dashed blue line) dynamical delta contributions.

up. The observed rise and fall times are $\sim$ 5 ns and timing resolution, measured in tagged photon experiments at MAX-lab, is $\sim$ 1 ns (σ). The target is highly insensitive to electrons and can be operated in bremsstrahlung beams of integrated intensity $\sim 10^8$ Hz. At MAX-lab the AT was placed in a maximum-intensity, tagged-photon beam, which produced greater than MHz rates on the focal-plane detectors but only a few kHz on the AT. Thus we expect that the counting rates in the focal-plane detector of the Glasgow-Mainz tagger will saturate well before the AT. Scintillations in

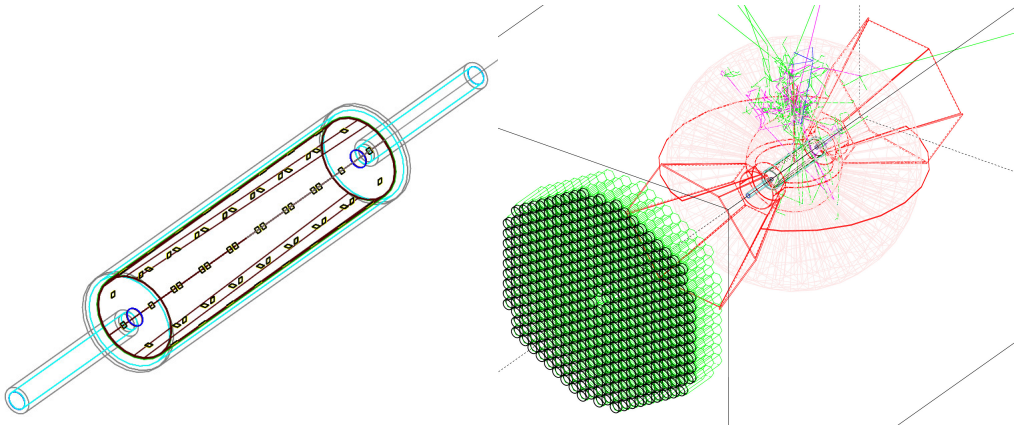

Figure 3: AT geometry rendered by the Geant-4 simulation. The left panel shows the AT itself, while the right panel shows the AT situated in the central cavity of the CB, with TAPS (green) covering forward angles.

He are approximately linear (i.e. there is little dependence of signal amplitude on ion velocity), so the AT counts low energy He ions efficiently. H ions (p, d, ^3H) are also detected, but they tend to deposit less energy in the target than He ions.

The combination of the CB and TAPS provides an electromagnetic calorimeter with excellent energy resolution and almost 4π coverage. The CB is the main detector, consisting of 672 NaI(Tl) crystals, which fit together into a spherical shape. The polar angle coverage (lab) is $20-160^\circ$ with full azimuthal coverage. The energy resolution for photons is $\sigma/E = 0.027/E^{1/4}$ (E in GeV) and angular resolution $2-3^\circ$. The hole in forward angle coverage is filled by TAPS, an array of 384 BaF_2 crystals arranged as a hexagonal wall. It covers lab angles up to 20° over the full 360° azimuth. Recently the inner two "rings" (about the photon beam axis) of BaF_2 crystals have been replaced by $PbWO_4$. These have ¼ the cross section of the BaF_2 crystals and also a much shorter pulse length. They are thus much less susceptible to rate-dependent losses at very small angles, where the atomic background is maximum.

3. Extraction of the ^{3}He Compton Signal

A Monte Carlo simulation based on Geant-4, which tracks the reaction products through a realistic model of the detector systems, is being employed to calculate the response to various reaction channels. Simulations have been made for incident photon energies $\omega = 80-200$ MeV. The correlation between the ^{3}He pulse height signal in the AT and the scattered photon in the CB is displayed in Fig.4. The Compton signal is obtained from:

$$P_{miss} = (P_\gamma + P_T - P_{\gamma'});\ E_{miss} = P_{miss} : E;\ E_{balance} = E_{miss} - E_{AT} \tag{3.1}$$

where P_{miss} is the missing four-momentum obtained if only the γ' is detected, E_{miss} is the missing kinetic energy derived from P_{miss}, and E_{AT} is the target kinetic energy obtained from the measured pulse height. Calculations have been made for coherent Compton scattering $\gamma + ^3He \rightarrow \gamma + ^3He$, and background processes which produce a neutral particle in the final state: quasi-free

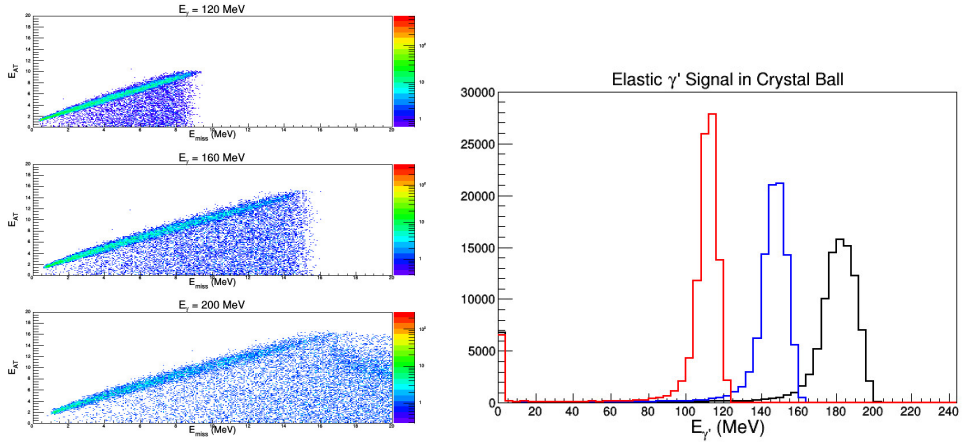

Figure 4: Left: correlation of the AT energy E_{AT} (from pulse height) with the γ' missing energy, measured in the CB for the $\gamma+^3He \rightarrow \gamma+^3He$ reaction at incident energies $E_\gamma = 120-200$ MeV. Right: the γ' energy signal in the CB for incident energies 120, 160 and 200 MeV.

$\gamma+^3He \rightarrow \gamma+p+d$, quasi-free $\gamma+^3He \rightarrow \gamma+p+p+n$ and breakup $\gamma+^3He \rightarrow n+p+p$. Coherent $\gamma+^3He \rightarrow \pi^0+He^3$, where E_γ exceeds π^0 threshold and a single decay photon only is detected, was also simulated.

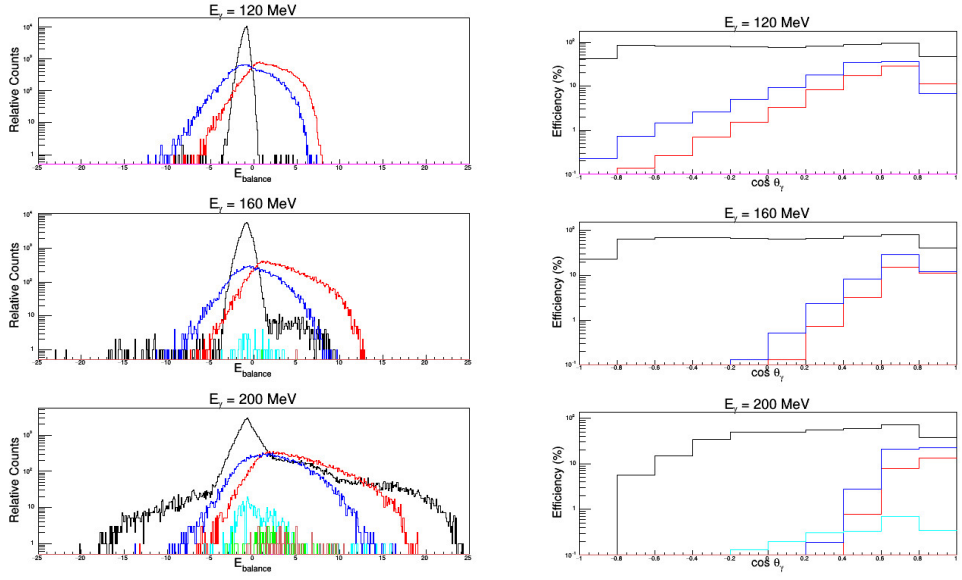

Figure 5: Left: kinetic-energy balance $E_{balance}$ (eq.3.1) for $\gamma+^3He \rightarrow \gamma+^3He$ (black line); $\gamma+^3He \rightarrow \gamma+p+d$ (blue line); $\gamma+^3He \rightarrow \gamma+n+p+p$ (red line); $\gamma+^3He \rightarrow \pi^0+^3He$ (cyan line). Right: acceptance for same reaction channels, colour code as left plot.

Fig.5:left compares the kinetic-energy balance $E_{balance}$ for coherent Compton scattering and the background processes. The coherent Compton signal has been selected by making cuts $-2.0 < E_{balance} < 1.0$ MeV and $E_{AT} > 1.0$ MeV, before calculating the acceptance (Fig.5:right) for the

channels listed above. The dip in Compton acceptance at forward angles results from the low energy of the recoiling ^{3}He, while at backward angles it is due to the lack of CB coverage at $\theta_{lab} > 160^\circ$. The present calculation suggests that there will be some contamination of the coherent signal by quasi-free Compton scattering, which will require a quantitative estimation.

4. Experimental Uncertainties

Estimates of the counting rate are based on experience of related experiments at Mainz and on acceptances calculated using the Monte Carlo simulation. An estimate of the precision which can be attained for the $\gamma + ^3He \rightarrow \gamma + ^3He$ differential cross section is shown in Fig. 6. Based on the currently available tagged-photon intensity, 200 hr of beam time produces statistical uncertainties varying from 4 - 7%. With the higher intensity tagged photon beam, these uncertainties will be a factor ~ 2 smaller. Systematic uncertainties arising from photon beam flux and the target thickness are expected to be $\sim 3\%$.

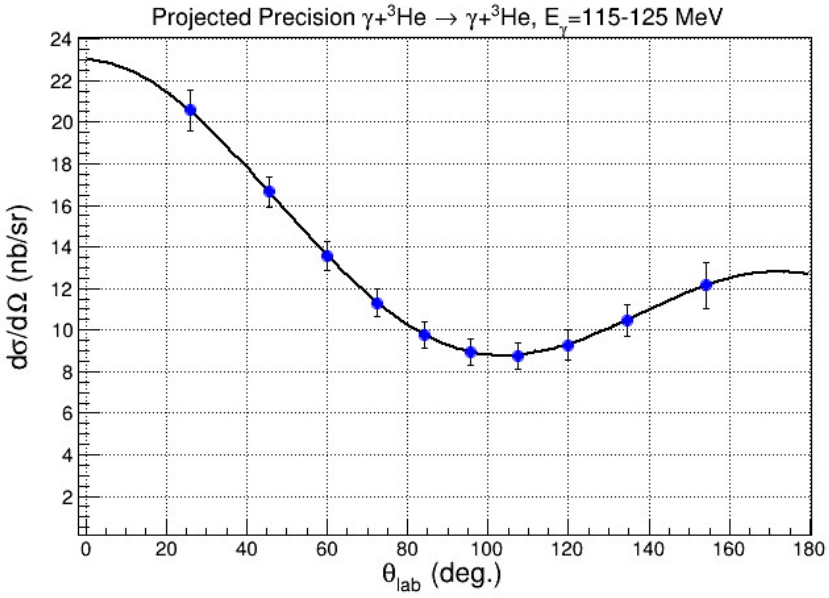

Figure 6: The projected precision for the $\gamma + ^3He \rightarrow \gamma + ^3He$ differential cross section at incident energy $E_\gamma = 115 - 125$ MeV. The full curve is the χEFT calculation by Shukla et al. The projected error bars show statistical uncertainties.

5. Summary

We will measure Compton scattering on ^{3}He (and ^{4}He) nuclei at Mainz, using tagged photons of energy $\omega = 80 - 200$ MeV. The scattered photons will be detected in the CB-TAPS segmented electromagnetic calorimeter, and the recoiling He nuclei in a high-pressure He-gas scintillator, which also acts as the experimental target. The motivation is to extract the isospin-averaged, scalar nucleon polarisabilities and, from these in turn, values for the neutron scalar polarisabilities. He

(Z=2) has the advantage over deuterium (Z=1) as an effective neutron target in that the Compton cross section is higher and the differential cross section is more sensitive to the values of the polarisabilities.

The extraction will depend on a Chiral Perturbation Theory fit to the differential cross section and already the prospect of new data has spawned new theoretical effort to extend the description of ^{3}He Compton scattering.

References

[1] M. Schumacher, Prog. Part. Nucl. Phys. 55, 567 (2005).

[2] H. W. Griesshammer, J. McGovern, D. R. Phillips and G. Feldman, Prog. Part. Nucl. Phys. 67 841-897 (2012).

[3] DOE/NSF Nuclear Science Advisory Committee, "The Frontiers of Nuclear Science – A Long-Range Plan", 2007.

[4] European Science Foundation, "Perspectives of Nuclear Physics in Europe – NuPECC Long-Range Plan 2010", 2010.

[5] P. P. Martel *et al*., Phys. Rev. Lett. 114, 112501 (2015).

[6] *Measurement of the Proton Spin Polarizabilities*, MAMI Proposal A2-05/-2012, Spokespersons: D. Hornidge, J.R,M. Annand, E.J. Downie and R. Miskimen.

[7] *Measurement of the Proton Scalar Polarizabilities*, MAMI Proposal A2-06/-2012, Spokespersons: E.J, Downie, J.R.M. Annand, D. Hornidge, and R. Miskimen.

[8] J.A. McGovern *et al*., Eur. Phys. J A 49, 12 (2013).

[9] J. Schmiedmayer *et al.*, Phys. Rev. Lett. 66, 1015 (1991).

[10] K.W. Rose, *et al*., Nuclear Phys. A 514, 621 (1990).

[11] N.R. Kolb, *et al.*, Phys. Rev. Lett. 85, 1388 (2000).

[12] K. Kossert *et al.*, Phys. Rev. Lett. 88, 162301 (2002).

[13] M.A. Lucas, Ph.D. Thesis, University of Illinois, 1994.

[14] M. Lundin, *et al.*, Phys. Rev. Lett. 90, 192501 (2003).

[15] D.L. Hornidge *et al*., Phys. Rev. Lett. 84, 2334 (2000).

[16] L. S. Myres *et al*., Phys. Rev. Lett. 113, 262506 (2014); Phys. Rev, C 92, 025203 (2015).

[17] L. S. Myers *et al*, Phys. Rev. C 90, 027603 (2014).

[18] J.R.M. Annand et al., *The Differential Cross Section for Compton Scattering on* ^{6}Li, Report to MAX-lab PAC, Sept. 2012.

[19] G. Bampa, W. Leidemann and H. Arenhovel, Phys. Rev. C 84, 034005 (2011).

[20] D. Shukla, A. Nogga and D. R. Phillips, Nucl. Phys. A 819, 98 (2009).

[21] H. Griesshammer et al., *Compton Scattering and Nucleon Polarizabilities in Chiral EFT: the Next Steps*, 8th Int. Workshop on Chiral Dynamics 2015, Pisa, June 2015.

[22] J.C. McGeorge *et al*., Eur. J. Phys A 37, 129 (2008).

[23] R. Al Jebali *et al*., arXiv:1503.05545, accepted for publication Eur. J. Phys. A.